Frequency Tuning of In-Plane Comb Drive MEMS Resonators Due to VO_2 Phase Transition

Juan Pastrana, *Graduate Student Member, IEEE*, David Torres, *Member, IEEE*, LaVern Starman, *Member, IEEE*, José Figueroa, Harris Hall, and Nelson Sepúlveda, *Senior Member, IEEE*

***Abstract*—This letter reports the thermal-mechanical tuning capability of an in-plane comb drive resonator using VO_2 phase transition material. By inducing the insulator-to-metal transition (IMT) using a heat conduction method, a shift of approximately 2% was observed. The frequency tuning was attributed to the induced stresses during the IMT. [2022-0200]**

***Index Terms*—Comb drive, resonators, frequency tuning, vanadium dioxide, tunable microelectromechanical systems, PolyMUMPs.**

I. Introduction

IN-PLANE resonators, such as comb drive structures, address issues that are intrinsic to out-of-plane devices, such as nonlinearity [1], low Q factor [2], and dynamic pull-in phenomena [3]. As a consequence, the incorporation of resonant frequency tuning capabilities is an attractive feature which can be obtained by inducing localized thermal stressing effects [4], by selective deposition of polysilicon over the beams [5], and by altering the suspension configuration using a DC pulling bias [6]. These approaches have resulted in 1%, 2%, and 50% shifts in frequency, respectively. The incorporation of phase-change materials presents an interesting alternative for tuning the frequency of MEMS resonators, where the crystallographic changes through the phase transition introduce the stress responsible for the changes in frequency by 2%.

This letter presents the thermal-mechanical tuning of an in-plane comb drive resonator based on thermally induced insulator-to-metal transition (IMT) of vanadium dioxide (VO_2). The phase transition occurs $\sim$ 68°C [7] changing from monoclinic (insulator) to rutile (metal) phase. The IMT introduces stresses to the resonator and shifts the resonant frequency.

II. Theoretical Analysis on Frequency Impact Due to VO_2 Transition

Fig. 1 shows a pictorial representation for the resonator used in this work. The standard folded-beam design [8] has been substituted by simple beams that directly connect the shuttle to the anchors. The analytical resonant frequency based on Rayleigh's method is given by [8],

$$f_0 = \frac{1}{2\pi}\sqrt{\frac{k}{(m_s + \frac{12}{35}m_b)}} \tag{1}$$

where k is the spring constant of the system, m_s and m_b are the mass of the shuttle and beams, respectively.

The proposed resonator considers polysilicon (PolySi) as the structural material, and a thin VO_2 film deposited over the shuttle. It has been previously shown that depositing VO_2 on thin beams results in out-of-plane displacements after release [9], which would be detrimental to the comb drive design. Although the Young's modulus changes during the IMT [10], here we consider to be the same value to simplify the analysis. After the deposition the overall mass of the resonator will increase, shifting f_0 to lower values. Each of the beams can be considered to have a fixed-guided boundary conditions at the anchor and shuttle connections, respectively. Since the actuation force is applied along the length of the shuttle (i.e. along the x-axis), the resulting spring constant of the system, k, is proportional to the Young's modulus (E) of the structure (mainly determined by the modulus of the main structural material), and inversely proportional to the effective length of the beams cubed (L^3). Following the fabrication process considered for this work -where a P-doped PolySi acts as the structural material- it is assumed the initial stress on the resonator's beam is compressive, yet the beams and shuttle do not exceed Euler's buckling criterion [11]. For a given material, the linear thermal expansion is described by,

$$L_{change} = L_{original}(1 + \alpha\Delta T) \tag{2}$$

where $L_{original}$ is the original length of the material, L_{change} is the material's length after heating, α is the thermal expansion coefficient (TEC) of the material, and ΔT is the difference between the material's deposition and room temperature. The major assumption in the following analysis is that all information concerning the crystallographic contraction between monoclinic (room temperature) and rutile (above 68°C) phases in VO_2 [12] is "embedded" in the TEC of VO_2. Table I shows thermal expansion coefficient values for PolySi, $VO_2(M)$, and $VO_2(R)$.

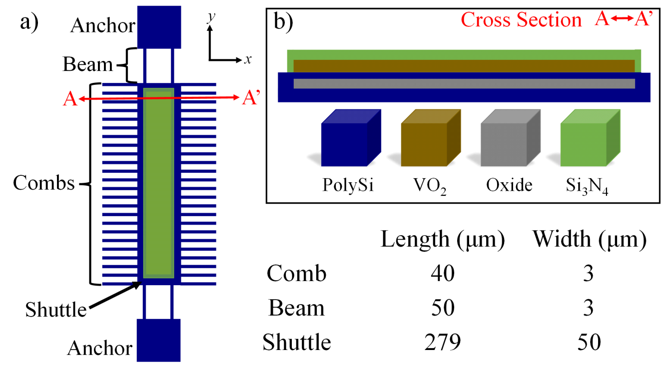

	Length (μm)	Width (μm)
Comb	40	3
Beam	50	3
Shuttle	279	50

Fig. 1. Pictorial representation of the bridge-shape Si_3N_4/VO_2-coated comb drive resonator. a) Shows a top view while b) shows a cross section.

Manuscript received 28 November 2022; revised 23 January 2023; accepted 24 January 2023. This work was supported in part by the National Science Foundation under Grant ECCS 1854750, in part by the Non-Academic Research Internships for Graduate Students (INTERN) program, and in part by the Cooperative Research and Development Agreement between the Air Force Research Laboratory Sensors Directorate (AFRL/RY) and Michigan State University enabled research collaboration under Grant CRADA 15-075-RY-01. Subject Editor R. T. Howe. *(Corresponding author: Nelson Sepúlveda.)*

Juan Pastrana and Nelson Sepúlveda are with the Department of Electrical and Computer Engineering, Michigan State University, East Lansing, MI 48824 USA (e-mail: nelsons@egr.msu.edu).

David Torres, LaVern Starman, and Harris Hall are with the Air Force Research Laboratory Sensors Directorate, Wright-Patterson Air Force Base, OH 45433 USA.

José Figueroa is with KBR Inc., Dayton, OH 45431 USA.

Color versions of one or more figures in this article are available at https://doi.org/10.1109/JMEMS.2023.3240076.

Digital Object Identifier 10.1109/JMEMS.2023.3240076

TABLE I
SUMMARY OF THERMAL EXPANSION COEFFICIENTS FOR MATERIALS USED IN THIS WORK

Material	Thermal Expansion Coefficient α (K^{-1})	Reference
$VO_2(M)$	$5.7\ x\ 10^{-6}$	[13]
$VO_2(R)$	$13.6\ x\ 10^{-6}$	[13]
$PolySi$	$4.4\ x\ 10^{-6}$	[14]

Deposition of VO_2 is done at $\sim$ 550°C where the rutile phase is stable. Noticing that $\alpha_{VO_2(R)} > \alpha_{PolySi}$, the polysilicon will expand less per degree temperature. Hence, as the temperature is returning to room temperature, the VO_2 film will want to contract at a faster rate, thus inducing a tensile stress in the now VO_2-coated shuttle, which works up to the beams. This is validated using Equation 2. However, this behavior happens only for temperature regions outside the phase transition. As the temperature crosses the phase transition during cooling to room temperature, the VO_2 crystal planes that are parallel to the substrate increase in area, adding compression to the unbuckled beam structure [12]. Conversely, when the structure is heated from room temperature across the phase transition, the crystal planes parallel to the surface contracts, thus adding tension to the structure. The beams in the comb-drive reported in this letter can be treated as being a fixed-fixed structures, where a force trying to reduce the length of the bridge structure (which is VO_2's effect during heating across the phase transition) translates to added tensile stress. This behavior has been observed before in VO_2-coated unbuckled bridge structures going through the phase during a heating cycle – i.e. increasing temperature, starting at room temperature– the bridge experiences an added tensile stress that causes an increase in the resonance frequency [9].

III. EXPERIMENTAL PROCEDURES

A. Fabrication Process

To validate the tuning capability shown in the previous section, the proposed resonator was fabricated utilizing Polysilicon Multi-User MEMS Processes (PolyMUMPs) from MEMSCAP. We followed the same terminology used in the PolyMUMPs handbook [15]. Briefly explained, the starting substrate is a heavily P-doped silicon wafer using phosphosilicate glass (PSG) in a standard diffusion furnace. After removing the PSG, a 600 nm layer of silicon nitride (Si_3N_4) is deposited by low pressure chemical vapor deposition (LPCVD) that serves as an electrical insulation layer. The following steps consist on the deposition and patterning of PolySi and Oxide layers (i.e., Poly0, Oxide1, Poly1, Oxide2, and Poly2) defining the comb drive resonators. The encapsulation of the oxide was done over the shuttle as seen in Figure 1b. The purpose of the encapsulated oxide is to add robustness to the center plate and prevent buckling of the structure.

The post-processing steps were carried out as follow. A deposition of $\sim$ 250 nm of VO_2 by pulsed laser deposition (PLD) was done using KrF laser operated at 10 Hz. A fluence of $\sim 2\frac{J}{cm^2}$ was used during a 45-minute deposition under oxygen atmosphere at a pressure of 15 mTorr. During the deposition, the substrate was heated to 550°C by a ceramic heater located behind the sample holder, and a 10-minute post annealing step was done at the same deposition conditions. After patterning and etching of the VO_2 by reactive ion etching [16], a 600 nm-thick Si_3N_4 layer was deposited at 300°C using physical enhanced chemical vapor deposition (PECVD), and patterned over the VO_2. This layer serves as a protective layer for the VO_2 during the subsequent structural release. The release etch was performed by immersing the die in a bath of room temperature 49% hydrofluoric acid (HF) for 3 minutes. Finally, the samples were supercritical CO_2 dried.

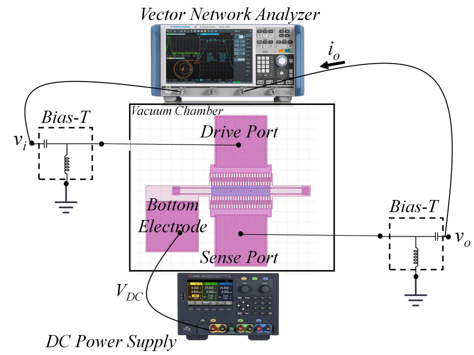

Fig. 2. Schematic illustrating the comb-drive resonator and the two-port testing configuration.

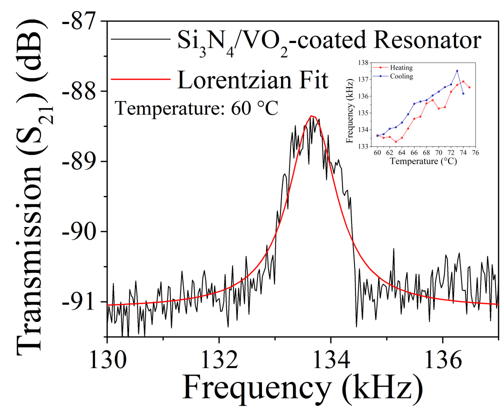

Fig. 3. Measured transmission for Si_3N_4/VO_2-coated resonator at 60°C. Inset shows extracted frequency values on a full heating-cooling cycle.

B. Experimental Setup

The experimental setup is shown in Figure 2. A vacuum chamber (Lakeshore TT-Prober System) with electrical feedthroughs and heating stage was used for electrical characterization as a function of temperature. A calibration curve for the heater was done by placing a thermocouple on the top of the heating stage, and the closed loop thermal feedback control was used and the temperature was allowed to reach steady state before each measurement, which were carried out at 3.5×10^{-7} Torr. To excite the resonator in its two-port configuration, a direct current (DC) bias voltage (V_{DC}) was applied to the structure, and an alternating (AC) current signal (v_i) was applied to the drive port; the output current (v_0) is measured at the sense port. The pair of bias tees protect the Vector Network Analyzer from the DC input. From preliminary tests, a 50 V_{DC} and power of 0 dBm were supplied to the device.

IV. RESULTS AND DISCUSSION

For baseline purposes, an identical (in 2D layout) but bare resonator underwent the Si_3N_4 deposition simultaneously with the VO_2-coated resonator described earlier. The effects of temperature on the resonant frequency, f_0, of the Si_3N_4-coated resonator are first discussed. To this end, electrical measurements were recorded in a temperature range from 60°C to 72°C in steps of 1°C. This temperature range is within the temperature window of the phase transition of VO_2. For each temperature point, a Lorentzian fit was applied to the observed resonance peak as shown in Figure 3, and

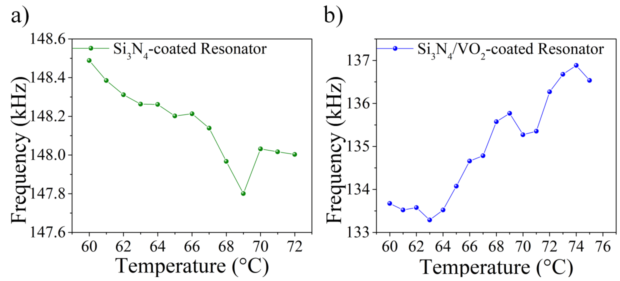

Fig. 4. Comparison between resonance frequencies of a) Si_3N_4-coated and b) Si_3N_4/VO_2-resonator as a function of increasing temperature.

Figure 4a shows the measured f_0 at each temperature. It is observed that as the temperature increases, f_0 decreases ($\sim$ 0.3% tuning). This behavior can be explained due to the beam structure since the beam would want to increase its length with increasing temperature. However, since the beams are fixed at both ends, this length increase is converted to compressive stress, which is known to cause a decrease in f_0 in such structures [9]. Furthermore, the frequency of the resonator is directly proportional to the stiffness constant as shown in Equation 1, which is dependent on E. An increase in temperature increases the atomic vibrations inside the material. Larger vibrations increase the atomic distances, decreasing the atomic forces. This translates as a "softening" effect of the material.

Figure 4b shows the results for the Si_3N_4/VO_2 -coated resonator. A decreasing trend in frequency is observed in the temperature range of $60-63$°C. This can be attributed to the added compressive stress and to the softening effect as it was previously explained. However, after 63°C (i.e., approaching the IMT) the measured frequency increases from 133.52 kHz to 136.27 kHz. As temperature approaches $\sim$ 68°C, the transformation of polycrystalline VO_2 from monoclinic to rutile is accompanied by a reduction in the area of the crystal planes (011) to (110), respectively. This has been discussed elsewhere where VO_2 has been deposited over silicon [16], [17].

Perhaps the most notable observation in the two compared comb-drive resonators (uncoated and VO_2-coated) is the different sign of the change in f_0 with increasing temperature. The decrease in f_0 with temperature of the uncoated structure is completely reversed with only the addition of a VO_2-coating. Although this phenomenon has been reported before in out-of-plane VO_2-based MEMS resonators, this letter reports the first observation for in-plane comb drive resonators.

V. Conclusion

The performance of a tunable VO_2-coated comb drive resonator across the IMT has been reported. The fabrication and electrical characterization as a function of increasing temperature show an increase of f_0 due to VO_2 phase transition of $\sim$ 2%. The increase in frequency was attributed to the tensile stress added by the VO_2 as it goes through its phase transition in a heating cycle. The induced stress was large enough to compensate for the decrease in f_0 when compared to the $\sim$ 0.3% tuning of the Si_3N_4-coated resonator.

Acknowledgment

This article was produced by the IEEE Publication Technology Group, Piscataway, NJ, USA.

References

[1] H. Farokhi, R. T. Rocha, A. Z. Hajjaj, and M. I. Younis, "Nonlinear damping in micromachined bridge resonators," *Nonlinear Dyn.*, vol. 111, no. 3, pp. 2311–2325, Feb. 2023.
[2] F. D. Bannon, J. R. Clark, and C. T.-C. Nguyen, "High-Q HF microelectromechanical filters," *IEEE J. Solid-State Circuits*, vol. 35, no. 4, pp. 512–526, Apr. 2000.
[3] A. H. Nayfeh, M. I. Younis, and E. M. Abdel-Rahman, "Dynamic pull-in phenomenon in MEMS resonators," *Nonlinear Dyn.*, vol. 48, pp. 153–163, Apr. 2007.
[4] T. Remtema and L. Lin, "Active frequency tuning for micro resonators by localized thermal stressing effects," *Sens. Actuators A, Phys.*, vol. 91, no. 3, pp. 326–332, Jul. 2001.
[5] D. Joachim and L. Lin, "Characterization of selective polysilicon deposition for MEMS resonator tuning," *J. Microelectromech. Syst.*, vol. 12, no. 2, pp. 193–200, Apr. 2003.
[6] I. Zine-El-Abidine and P. Yang, "A tunable mechanical resonator," *J. Micromech. Microeng.*, vol. 19, no. 12, Dec. 2009, Art. no. 125004.
[7] F. J. Morin, "Oxides which show a metal-to-insulator transition at the Neel temperature," *Phys. Rev. Lett.*, vol. 3, pp. 34–36, Jul. 1959.
[8] W. C. Tang, T.-C. H. Nguyen, M. W. Judy, and R. T. Howe, "Electrostatic-comb drive of lateral polysilicon resonators," *Sens. Actuators A, Phys.*, vol. 21, nos. 1–3, pp. 328–331, 1990.
[9] E. Merced, R. Cabrera, N. Dávila, F. E. Fernández, and N. Sepúlveda, "A micro-mechanical resonator with programmable frequency capability," *Smart Mater. Struct.*, vol. 21, no. 3, Mar. 2012, Art. no. 035007.
[10] N. Sepúlveda, A. Rúa, R. Cabrera, and F. Fernández, "Young's modulus of VO_2 thin films as a function of temperature including insulator-to-metal transition regime," *Appl. Phys. Lett.*, vol. 92, no. 19, May 2008, Art. no. 191913.
[11] J. M. Gere and S. P. Timoshenko, *Mechanics of Materials*. Marshall St, Arvada, CO, USA: Wadsworth, 1984.
[12] A. Rúa, F. E. Fernández, and N. Sepúlveda, "Bending in VO_2-coated microcantilevers suitable for thermally activated actuators," *J. Appl. Phys.*, vol. 107, no. 7, Apr. 2010, Art. no. 074506.
[13] D. Kucharczyk and T. Niklewski, "Accurate X-ray determination coefficients of VO_2 near the transition temperature," *J. Appl. Crystallogr.*, vol. 12, pp. 370–373, Aug. 1979.
[14] H. Tada et al., "Thermal expansion coefficient of polycrystalline silicon and silicon dioxide thin films at high temperatures," *J. Appl. Phys.*, vol. 87, no. 9, pp. 4189–4193, 2000.
[15] A. Cowen, B. Hardy, R. Mahadevan, and S. Wilcenski, "PolyMUMPs design handbook: A MUMPs process," MEMSCAP Inc., Durham, NC, USA, Tech. Rep., Revision 13, 2011.
[16] D. Torres et al., "VO_2-based MEMS mirrors," *J. Microelectromech. Syst.*, vol. 25, no. 4, pp. 780–787, May 2016.
[17] A. Rúa, F. Fernández, and N. Sepúlveda, "Study of the resonant frequencies of silicon microcantilevers coated with vanadium dioxide films during the Insulator-to-Metal transition," *ECS Meeting Abstr.*, vols. 107, Jul. 2010, Art. no. 053528.